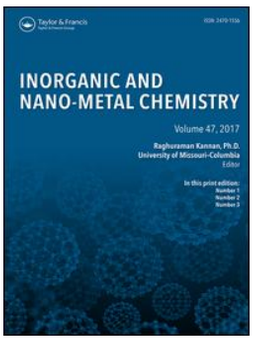

Inorganic and Nano-Metal Chemistry

ISSN: (Print) (Online) Journal homepage: https://www.tandfonline.com/loi/lsrt21

Synthesis, crystal structure and antibacterial activity of a heterometallic tetranuclear Cd_2Tb_2 complex derived from 5-chloro-2-(3-ethoxy-2-hydroxybenzylideneamino)phenol

Shao-Song Qian

To cite this article: Shao-Song Qian (2021): Synthesis, crystal structure and antibacterial activity of a heterometallic tetranuclear Cd_2Tb_2 complex derived from 5-chloro-2-(3-ethoxy-2-hydroxybenzylideneamino)phenol, Inorganic and Nano-Metal Chemistry, DOI: 10.1080/24701556.2021.1897616

To link to this article: https://doi.org/10.1080/24701556.2021.1897616

Published online: 17 Mar 2021.

INORGANIC AND NANO-METAL CHEMISTRY
https://doi.org/10.1080/24701556.2021.1897616

Synthesis, crystal structure and antibacterial activity of a heterometallic tetranuclear Cd_2Tb_2 complex derived from 5-chloro-2-(3-ethoxy-2-hydroxybenzylideneamino)phenol

Shao-Song Qian

School of Life Sciences, Shandong University of Technology, Zibo, P.R. China

ABSTRACT

A new heterometallic tetranuclear complex $[Cd_2Tb_2L_4(CH_3COO)_2(DMF)_2]$ was prepared from the Schiff base 5-chloro-2-(3-ethoxy-2-hydroxybenzylideneamino)phenol (H_2L). The complex was characterized by IR and UV–vis spectra, as well as single crystal X-ray determination. The Cd atoms are in octahedral coordination with O_5N donor set, and the Tb atoms are in square-antiprismatic coordination with O_7N donor set. The Cd and Tb atoms are bridged by phenolate oxygen and acetate groups. The Schiff base and the complex showed good antibacterial activities against the bacteria *Escherichia coli*, *Pseudomonas aeruginosa,* and *Salmonella typhi*.

ARTICLE HISTORY
Received 25 August 2020
Accepted 1 December 2020

KEYWORDS
Schiff base; Cd-Tb complex; heteronuclear complex; crystal structure; antibacterial activity

Introduction

Schiff base ligands are a favorite choice for the construction of metal complexes with versatile structures and widely applications.[1–4] Polynuclear complexes of transition metal atoms have attracted much attention due to their interesting catalytic, magnetic, and biological activities.[5–8] Some cadmium complexes and terbium complexes are reported to have various biological activities like antibacterial.[9–12] Generally, multi-dentate ligands with suitable configuration are used to construct metal complexes with versatile structures. The tetra-dentate Schiff bases with the basal skeleton 2-(hydroxybenzylideneamino)phenol (HBP) have received particular interest in constructing polynuclear complexes.[13–17] Although coordination of HBP and its derivatives to nickel(II), manganese(II), zinc(II), and copper(II) has been reported, this type of ligands remains little investigated. The reported heterometallic polynuclear complexes of such Schiff bases are focused on their magnetic properties. Considering the good biological activities of Schiff base complexes, herein, we report a new heterometallic tetranuclear complex, $[Cd_2Tb_2L_4(CH_3COO)_2(DMF)_2]$, where L is the dianionic form of 5-chloro-2-(3-ethoxy-2-hydroxybenzylideneamino)phenol (H_2L; Scheme 1). The preliminary study on the antibacterial activities was also reported.

Experimental

Materials and measurements

All starting materials were of analytical reagent grade and were used as received without further purification. All reactions were carried out under aerobic conditions. ^1H and ^{13}C NMR spectra were recorded on a Bruker DRX-500 NMR spectrometer; chemical shifts are referenced to residual solvent peaks (with respect to TMS = δ 0 ppm). FTIR spectra were recorded on a Bruker AXS TENSOR-27 instrument with KBr pellets. UV–vis spectra were recorded on a Lambda 35 spectrophotometer.

Synthesis of 5-chloro-2-(3-ethoxy-2-hydroxybenzylideneamino)phenol (H_2L)

A solution of 2-amino-4-chlorophenol (0.72 g, 5.0 mmol) in MeOH (20 mL) was added to a stirred solution of and 3-ethoxysalicylaldehyde (0.83 g, 5.0 mmol) in MeOH (20 mL) and the resulting solution was stirred at room temperature for 1 h. The solvent was evaporated to give orange precipitate, which was recrystallized from ethanol to form crystalline product.

Yield: 1.1 g (76%). Elemental analysis: Calcd for $C_{15}H_{14}ClNO_3$: C, 61.76; H, 4.84; N, 4.80. Found: C, 61.57; H, 4.93; N, 4.72. ^1H NMR (500 MHz, DMSO-*d*6) δ/ppm: 13.70 (s, 1H, OH), 10.01 (s, 1H, OH), 8.98 (s, 1H, CH = N), 7.49 (s, 1H, ArH), 7.20–7.15 (m, 2H, ArH), 7.10 (d, 1H, ArH), 6.97 (d, 1H, ArH), 6.86 (t, 1H, ArH), 4.07 (q, 2H, CH_2), 1.35 (t, 3H, CH_3). ^{13}C NMR (126 MHz, DMSO-*d*6) δ/ppm: 162.96, 151.68, 150.11, 147.17, 135.84, 127.30, 124.13, 123.08, 119.33, 119.10, 118.18, 117.76, 116.99, 64.09, 14.77. IR (KBr, cm^{-1}): 3436 br, 1634s, 1598s, 1505s, 1431 w, 1353 m, 1290 w, 1245 m, 1209s, 1172 w, 1079 w, 1006 m, 902 m 812 w, 745 m. UV–vis λ_{max}/nm (1.02×10^{-5} mol L^{-1}, MeOH; ε, L mol^{-1} cm^{-1}): 263 (22700), 298 (10120), 345 (8750).

CONTACT Shao-Song Qian sdutqss@163.com School of Life Sciences, Shandong University of Technology, Zibo 255049, P.R. China.

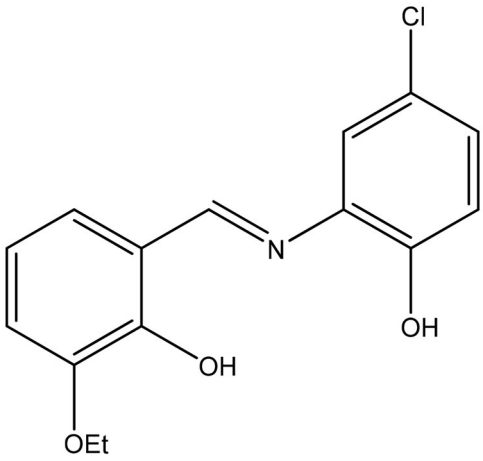

Scheme 1. H_2L.

Table 1. Crystallographic and refinement data for the complex.

Formula	$C_{70}H_{68}Cd_2Cl_4N_6O_{18}Tb_2$
Formula weight	1965.74
T (K)	298(2)
Crystal system	Triclinic
Space group	$P\bar{1}$
a (Å)	10.6911(12)
b (Å)	12.4497(13)
c (Å)	15.7119(10)
α (°)	85.623(1)
β (°)	71.148(1)
γ (°)	74.672(1)
V (Å^3)	1909.6(3)
Z	1
D_{calc} (g cm^{-3})	1.709
μ (Mo Kα) (mm^{-1})	2.588
F(000)	968
Measured reflections	10713
Unique reflections	6966
Observed reflections ($I \geq 2\sigma(I)$)	5099
Parameters	462
Restraints	0
Goodness of fit on F^2	1.008
R_1, wR_2 $[I \geq 2\sigma(I)]^a$	0.0596, 0.1497
R_1, wR_2 (all data)^a	0.0843, 0.1696

$^aR_1 = F_o - F_c/F_o$, $wR_2 = [\sum w(F_o^2 - Fc^2)/\sum w(F_o^2)^2]^{1/2}$

Synthesis of $[Cd_2Tb_2L_4(CH_3COO)_2(DMF)_2]$

A solution of triethylamine (0.65 mL, 0.30 mmol) was added to the methanolic solution (10 mL) of H_2L (29 mg, 0.10 mmol). The reaction mixture was stirred for 30 min. Then, solid terbium nitrate hexahydrate (45 mg, 0.10 mmol) was added to the above mixture, and the resulting solution was stirred for 1 h. Solid nickel acetate tetrahydrate (25 mg, 0.10 mmol) was added and further stirred for 1 h. A total of 5 mL *N*,*N*-dimethylformamide was subsequently added, and the reaction mixture was filtered and then left unperturbed to allow the slow evaporation of the solution. Deep green block single crystals, suitable for X-ray diffraction analysis, were obtained after 12 days. These crystals were collected by filtration, washed with cold methanol, and dried in air.

Yield: 1.1 g (76%). Elemental analysis: Calcd for $C_{70}H_{68}Cd_2Cl_4N_6O_{18}Tb_2$: C, 42.77; H, 3.49; N, 4.28. Found: C, 42.96; H, 3.61; N, 4.15. IR (KBr, cm^{-1}): 3587 w, 3531 w, 1642s, 1598s, 1543 m, 1480s, 1433s, 1381 m, 1310 m, 1282 m, 1246s, 1213s, 1108 w, 1078 w, 1012 w, 927 w, 896 w, 845 w, 742 w, 676 m, 657 w, 588 w, 545 w, 459 w. UV–vis λ_{max}/nm (1.07×10^{-5} mol L^{-1}, MeOH; ε, L mol^{-1} cm^{-1}): 230 (20600), 296 (8135), 373 (7620), 425 (7250).

Table 2. Selected bond distances (Å) and angles (°) for the complex.

Tb1-O1	2.206(6)	Tb1-O4	2.332(6)
Tb1-O8	2.356(7)	Tb1-O2	2.391(6)
Tb1-O5A	2.415(6)	Tb1-O9	2.475(8)
Tb1-N1	2.533(8)	Tb1-O6	2.565(6)
Cd1-O2	2.215(5)	Cd1-N2	2.227(7)
Cd1-O4	2.229(6)	Cd1-O5	2.264(6)
Cd1-O7	2.268(7)	Cd1-O2A	2.563(5)
O1-Tb1-O4	149.5(2)	O1-Tb1-O8	113.8(3)
O4-Tb1-O8	83.1(2)	O1-Tb1-O2	135.9(2)
O4-Tb1-O2	71.8(2)	O8-Tb1-O2	73.4(2)
O1-Tb1-O5A	84.3(2)	O4-Tb1-O5A	94.84(19)
O8-Tb1-O5A	146.6(3)	O2-Tb1-O5A	74.30(19)
O1-Tb1-O9	75.0(3)	O4-Tb1-O9	88.2(3)
O8-Tb1-O9	70.9(3)	O2-Tb1-O9	140.8(2)
O5-Tb1-O9A	142.5(2)	O1-Tb1-N1	72.7(2)
O4-Tb1-N1	137.4(2)	O8-Tb1-N1	78.9(3)
O2-Tb1-N1	66.1(2)	O5-Tb1-N1A	80.5(2)
O9-Tb1-N1	120.8(3)	O1-Tb1-O6	87.7(2)
O4-Tb1-O6	62.36(19)	O8-Tb1-O6	127.0(2)
O2-Tb1-O6	124.02(18)	O5-Tb1-O6A	79.2(2)
O9-Tb1-O6	69.2(3)	N1-Tb1-O6	152.9(2)
O2-Cd1-N2	158.2(2)	O2-Cd1-O4	77.1(2)
N2-Cd1-O4	83.9(2)	O2-Cd1-O5	116.8(2)
N2-Cd1-O5	75.3(2)	O4-Cd1-O5	148.6(2)
O2-Cd1-O7	87.1(2)	N2-Cd1-O7	106.0(2)
O4-Cd1-O7	96.9(3)	O5-Cd1-O7	111.2(3)
O2-Cd1-O2A	80.6(2)	N2-Cd1-O2A	86.2(2)
O4-Cd1-O2A	81.86(19)	O5-Cd1-O2A	73.63(19)
O7-Cd1-O2A	167.6(2)		

Crystal structure determinations

A suitable single crystal with dimensions of $0.11 \times 0.08 \times 0.08$ mm^3 for the complex was selected for single-crystal X-ray diffraction analysis. Crystallographic data were collected at a temperature of 298(2) K on a Bruker Apex II CCD diffractometer with graphite-monochromated Mo Kα radiation ($\lambda = 0.71073$ Å). Data processing was accomplished with the SAINT processing program.[18] The structure was solved by direct methods and refined on F^2 by full-matrix least squares using SHELXTL.[19] The locations of the heaviest atoms (Cd, Tb) were easily determined, and the O, N, Cl, and C atoms were subsequently determined from the difference Fourier maps. The non-H atoms were refined isotopically. The crystal data and refinement parameters are listed in Table 1. Selected bond lengths and angles of the complex are summarized in Table 2.

Antibacterial assay

Qualitative determination of antibacterial activity was done using the disk diffusion method. Suspensions in sterile peptone water from 24 h culture of microorganisms were adjusted to 0.5 McFarland. Muller–Hinton Petri dishes of 90 mm were inoculated using these suspensions. Paper disks (6 mm in diameter) containing 10 μL of the substance to be tested (at a concentration of 2048 μg/mL in DMSO) were

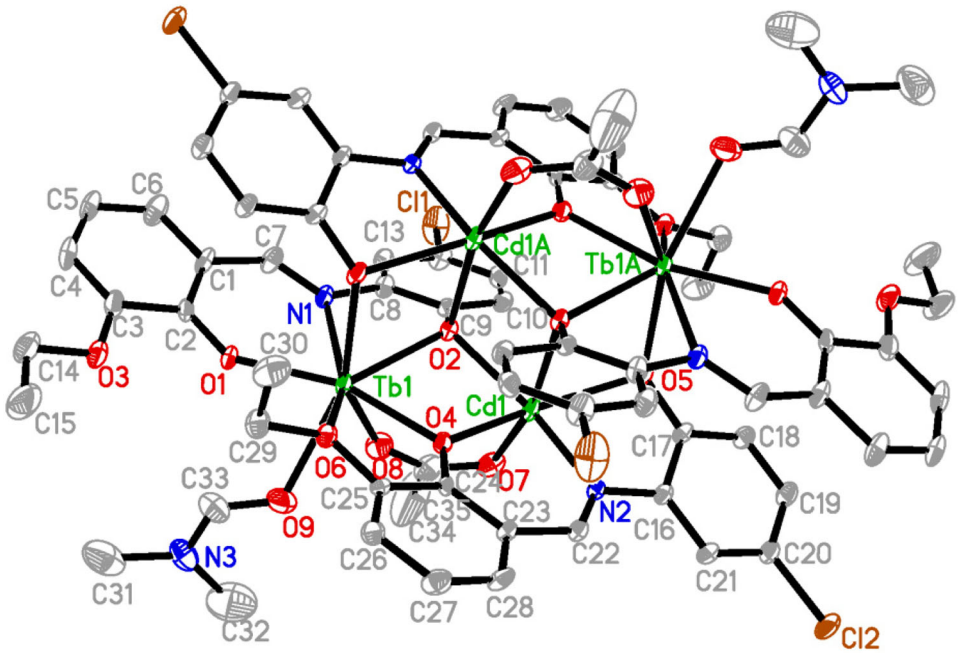

Figure 1. Molecular structure of the complex, showing the crystallographic numbering scheme. Displacement ellipsoids are drawn at the 30% probability level and H atoms are omitted for clarity. Atoms labeled with the suffix A and those unlabeled are related to the symmetry operation 1 – *x*, 2 – *y*, – *z*.

placed in a circular pattern in each inoculated plate. Incubation of the plates was done at 37 °C for 18–24 h. DMSO impregnated disks were used as negative controls. Toxicity tests of the solvent, DMSO, showed that the concentrations used in antibacterial activity assays did not interfere with the growth of the microorganisms. Reading of the results was done by measuring the diameters of the inhibition zones generated by the test substance. Penicillin was used as a reference.

Determination of MIC was done using the serial dilutions in liquid broth method. The materials used were 96-well plates, suspensions of microorganism, Muller-Hinton broth and stock solutions of each substance to be tested (2048 μg/mL in DMSO). The following concentrations of the substances to be tested were obtained in the 96-well plates: 1024, 512, 256, 128, 64, 32, 16, 8, 4, 2, and 1 μg/mL. After incubation at 37 °C for 18–24 h, the MIC for each tested substance was determined by microscopic observation of microbial growth. It corresponds to the well with the lowest concentration of the tested substance where microbial growth was clearly inhibited.

Results and discussion

Chemistry

To the best of our knowledge, although some complexes derived from similar Schiff bases as H_2L have been reported,[13–17] the crystal structure of the present complex is new. The Schiff base H_2L was obtained as orange product from the condensation reaction of 2-amino-4-chlorophenol with 3-ethoxysalicylaldehyde. The orange color arises from a broad band (λ_{max} = 345 nm) in the electronic absorption spectrum that extends into the visible region.[16]

The reaction of H_2L with terbium nitrate hexahydrate and nickel acetate tetrahydrate in the presence of triethylamine in a mixture of DMF and MeOH resulted in the green solution of the complex. The crystals of the complex were obtained by slow evaporation of the solution in air.

Structure description of $[Cd_2Tb_2L_4(CH_3COO)_2(DMF)_2]$

The molecular structure of the complex is shown in Figure 1. The complex crystallizes in the triclinic space group *P*\bar1, and with $Z = 1$ such that the molecule has centrosymmetric site symmetry in the crystal. The complex is composed of four metal atoms, four Schiff base ligands, two acetate bridging ligands, and two DMF terminal ligands. The Cd atom has adopted a slightly distorted octahedral geometry with an O_5N donor set, while the Tb atom has a distorted square antiprismatic geometry with an O_7N donor set. The Cd atom is chelated by the imino N and two phenolate atoms of one of the two independent Schiff base ligands in the structure, with these two phenolate O atoms each forming μ_2-bridges from the chelated Cd to different Tb atoms. The other independent Schiff base ligand coordinates rather differently, with one phenolate O atom chelating a Tb atom. The vanillin-derived phenolate O atom coordinates to the Tb atom, and not coordinates to other metal atoms. The amino phenolate O atom, by contrast, forms a μ_3-bridge over a Cd_2Tb triangle. Two such triply bridging oxygens coordinate to each Cd atom, with an acetate ligand coordinating through oxygen completing the O_5N environment of each Cd center. Each Tb atom is ligated by

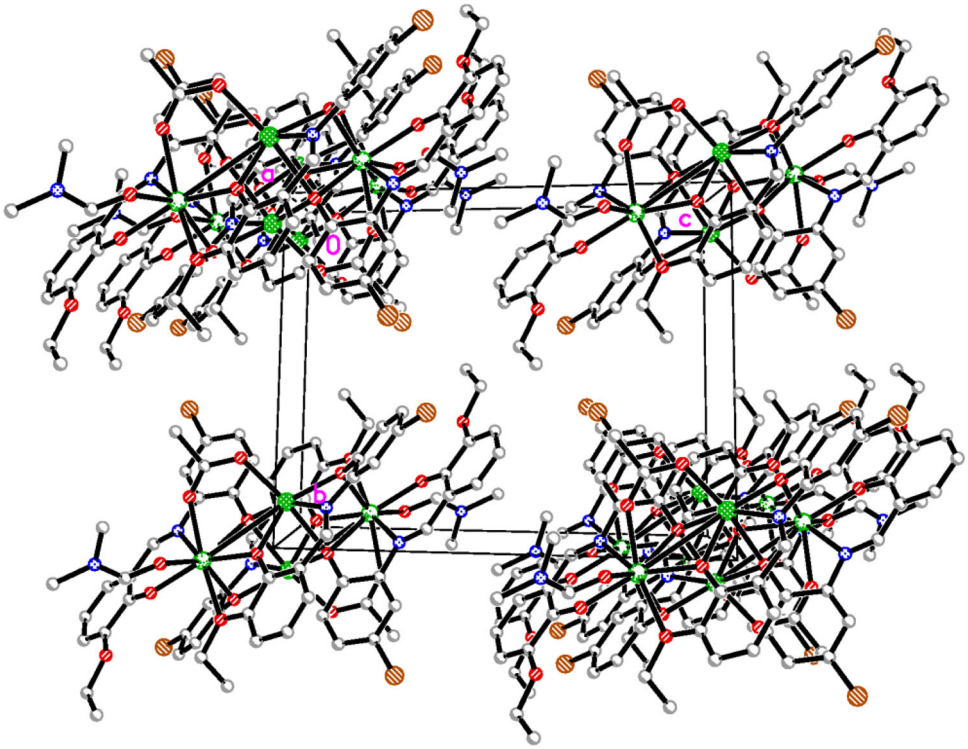

Figure 2. The molecular packing structure of the complex, viewed along the *a* axis.

the ONO donor set of one Schiff base ligand, and the OO donor set of the other independent Schiff base ligand from opposite directions, filling five coordination sites in a distorted pentagonal planar geometry. The sixth coordination site is occupied by a μ_2-phenolate O atom from a third Schiff base ligand, and the seventh and eighth sites are filled by the other O atom of the acetate ligand, and the O atom of the DMF ligand. The core of the complex can be described in terms of the well-known defect-dicubane or butterfly topology with two Cd atoms in the body positions and each Tb atom in the wing positions.[14] The metal atoms of Cd_2Tb_2 core are each bridged by μ_2-phenolate O atoms from two symmetry-related Schiff base ligands, while the two other Schiff base ligands form μ_3-bridges over the two Cd_2Tb triangles with O_2 atom displaced by 0.925(2) Å out of the Cd_2Tb plane, on opposite sides of the strictly planar Cd_2Tb_2 core. Similar tetranuclear topology can be found in some nickel or nickel and rare earth metal complexes.[20–22] Each acetate ligand bridges the terminal metal and central metal in a *syn-syn* fashion.

The crystal structure is shown as Figure 2. There are weak $\pi\cdots\pi$ interactions among the molecules with centroid to centroid distances of 3.02–4.83 Å [$Cg1\cdots Cg4 = 3.024(4)$ Å, $Cg1\cdots Cg9 = 4.826(4)$ Å, $Cg4\cdots Cg4^{iv} = 4.824(4)$ Å, $Cg4\cdots Cg7^{v} = 3.491(4)$ Å, $Cg4\cdots Cg9^{vi} = 3.853(4)$ Å, $Cg6\cdots Cg8 = 3.645(4)$ Å, $Cg7\cdots Cg9 = 3.657(4)$ Å, $Cg9\cdots Cg9^{vii} = 4.390(4)$ Å; *Cg*1, *Cg*4, *Cg*6, *Cg*7, *Cg*8 and *Cg*9 are the centroids of Cd1-O2-Cd1A-O2A, Cd1-O4-C24-C23A-C22A-N2A, C1-C2-C3-C4-C5-C6, C8-C9-C10-C11-C12-C13, C16-C17-C18-C19-C20-C21 and C23-C28-C27A-C26A-C25A-C24A rings, respectively; symmetry codes: iv: – *x*, 2 – *y*, – *z*; v: 1 – *x*, 2 – *y*, – *z*; vi: −1 + *x*, *y*, *z*; vii: 2 – *x*, 2 – *y*, – *z*].

IR and UV–vis spectra

The IR spectrum of H_2L and the complex provide information about the metal-ligand bonding. The assignments are based on the typical group frequencies. The weak and broad absorptions in the range of 3400–3600 cm^{-1} can be assigned to the O-H vibrations of phenol groups or solvent molecules. The spectra of the compounds show several weak bands corresponding to aromatic and aliphatic C-H stretching in the range of 2810–3015 cm^{-1}. The strong absorption band at 1634 cm^{-1} in the spectrum of H_2L is assigned to the azomethine group, ν(C = N). The band is observed at 1642 cm^{-1} in the spectrum of the complex, indicating the coordination through the imino N atom. The Ar-O stretching band at 1245 cm^{-1} in the spectrum of the free Schiff base H_2L shift to lower frequency by 32 cm^{-1} in the complex (1213 cm^{-1}), upon complexation with metals.[23,24] The weak bands at 588, 545, and 459 cm^{-1} for the complex can be assigned to ν(M-O).[23,25] The difference between ν_{asym}(COO) (1598 cm^{-1}) and ν_{sym}(COO) (1433 cm^{-1}) ($\Delta\nu = 165$ cm^{-1}), which reflects the bidentate bridging coordination mode of the acetate ligand.[24,26]

In the UV–vis spectrum of H_2L, there are three π–π^* transitions at 263 nm, 298 nm, and 345 nm. For the spectrum of the complex, a new band at 425 nm can be ascribed to LMCT excitation. The bands at 230 and 296 nm due to intra-ligand transitions are observed.[20]

^{1}H and ^{13}C NMR spectra of H_2L

The ^{1}H NMR spectrum of H_2L displays triplet signal at 1.35 ppm, which is assigned to protons of the CH_3 group, and the quartet signal at 4.07 ppm assigned to protons of

Table 3. Antimicrobial activities of the compounds as MIC values (μg/mL).

	H_2L	the complex	Penicillin
Escherichia coli	32	8	230
Pseudomonas aeruginosa	16	8	65
Salmonella typhi	32	4	250
Staphylococcus aureus	64	32	12

the CH_2 group. The signals at 6.86–7.49 ppm are assigned to the aromatic protons. The singlet signal at 8.98 ppm is assigned to CH = N group. The singlet signals at 13.70 and 10.01 ppm are assigned to the OH groups. The ^{13}C NMR spectrum of H_2L displays signal at 14.77 ppm, which is assigned to the carbon of the CH_3 group, and the signal at 64.09 ppm assigned to the carbon of the CH_2 group. The signal at 162.96 ppm is assigned to the carbon of the CH = N group. All the other signals are ascribed to the carbon atoms of the aromatic rings.

Antibacterial activity

The antibacterial microbial activities of the compounds against the organisms *Escherichia coli*, *Pseudomonas aeruginosa*, *Salmonella typhi,* and *Staphylococcus aureus* are summarized in Table 3. The results show that the Schiff base H_2L has effective activities against *Escherichia coli*, *Pseudomonas aeruginosa,* and *Salmonella typhi*, and weak activity against *Staphylococcus aureus*. The complex has in general higher activities against all the bacteria than the free Schiff base. Both the Schiff base and the complex have higher activities against *Escherichia coli*, *Pseudomonas aeruginosa,* and *Salmonella typhi* when compared to the Penicillin. Interestingly, the complex has the most effective activity against *Salmonella typhi* with the MIC value of 4 μg/mL. Moreover, the complex has strong activities against *Escherichia coli* and *Pseudomonas aeruginosa* with MIC values of 8 μg/mL.

Such increased activity of the complex than the free Schiff base compound can be explained on the basis of chelation theory.[27] On chelation, the polarity of the metal ion will be reduced to a great extent due to the overlap of the ligand orbital. Furthermore, it increases the delocalization of π-electrons over the whole chelate ring and enhances the lipophilicity of the complexes.[25] This increased lipophilicity leads to breakdown of the permeability barrier of the cell and thus retards the normal cell processes.[28]

Conclusions

A new centrosymmetric heterometallic tetranuclear Cd^{II}-Tb^{III} complex with a Cd_4Tb_4 cubane core was synthesized from the Schiff base 5-chloro-2-(3-ethoxy-2-hydroxybenzylideneamino)phenol. The single crystal structure of the complex indicates that the Schiff base coordinates to the metal atoms through the four donor atoms. The complex has interesting antibacterial activities against the bacteria *Escherichia coli*, *Pseudomonas aeruginosa,* and *Salmonella typhi*.

Disclosure statement

No potential conflict of interest was reported by the authors.

Supplementary data

CCDC 2006772 contains the supplementary crystallographic data for this paper. These data can be obtained free of charge via http://www.ccdc.cam.ac.uk/conts/retrieving.html, or from the Cambridge Crystallographic Data Centre, 12 Union Road, Cambridge CB2 1EZ, UK; fax: (+44) 1223-336-033; or e-mail: deposit@ccdc.cam.ac.uk.

References

1. Zhang, L.; Gao, W.; Wu, Q.; Su, Q.; Zhang, J.; Mu, Y. Synthesis and Characterization of Chiral Trinuclear Cobalt and Nickel Complexes Supported by Binaphthol-Derived Bis(Salicylaldimine) Ligands. *J. Coord. Chem.* **2013**, *66*, 3182–3192. DOI: 10.1080/00958972.2013.830716.
2. Xi, X.; Fang, Y.; Dong, T.; Cui, Y. Bottom-up Assembly from a Helicate to Homochiral Micro- and Mesoporous Metal-Organic Frameworks. *Angew. Chem. Int. Ed. Engl.* **2011**, *50*, 1154–1158. DOI: 10.1002/anie.201004885.
3. Mandal, A.; Dasgupta, S.; Adhikary, A.; Samanta, D.; Zangrando, E.; Das, D. Synthesis of Mn_3O_4 Nanozymes from Structurally Characterized Phenoxazinone Synthase Models Based on Manganese(III) Schiff Base Complexest. *Dalton. Trans.* **2020**, *49*, 5999–6011. DOI: 10.1039/d0dt00355g.
4. Consiglio, G.; Oliveri, I. P.; Cacciola, S.; Maccarrone, G.; Failla, S.; di Bella, S. Dinuclear Zinc(II) Salen-Type Schiff-Base Complexes as Molecular Tweezers. *Dalton Trans.* **2020**, *49*, 5121–5133. DOI: 10.1039/d0dt00494d.
5. Keypour, H.; Azizi, E.; Mahmoudabadi, M.; Salehzadeh, S.; Hajibabaei, F.; Gable, R. W. Synthesis and Crystal Structure of Manganese(III), Zinc(II) and Cadmium(II) Complexes Based on a Symmetrical Macroacyclic Schiff Base Ligand Containing Piperazine Moiety, DNA Binding Studies of Complexes. *Transit. Met. Chem.* **2020**, *45*, 227–235. DOI: 10.1007/s11243-019-00374-8.
6. Adak, P.; Mondal, A.; Chattopadhyay, S. K. Manganese(II) Complex of an Oxygen-Nitrogen Donor Schiff Base Ligand Showing Efficient Catechol Oxidase Activity: Synthesis, Spectroscopic and Kinetic Study. *New J. Chem.* **2020**, *44*, 3748–3754. DOI: 10.1039/C9NJ04591K.
7. Nagalakshmi, V.; Nandhini, R.; Venkatachalam, G.; Balasubramani, K. Synthesis and Characterization of New Ruthenium(III) Complexes Derived from Fluoreneamine-Based Schiff Base Ligands and Their Catalytic Activity in Transfer Hydrogenation of Ketones. *J. Coord. Chem.* **2020**, *73*, 206–216. DOI: 10.1080/00958972.2020.1718665.
8. Basak, D.; van Leusen, J.; Gupta, T.; Kogerler, P.; Bertolasi, V.; Ray, D. Unusually Distorted Pseudo-Octahedral Coordination Environment around Co^{II} from Thioether Schiff Base Ligands in Dinuclear [CoLn] (Ln = La, Gd, Tb, Dy, Ho) Complexes: Synthesis, Structure, and Understanding of Magnetic Behavior. *Inorg. Chem.* **2020**, *59*, 2387–2405. DOI: 10.1021/acs.inorgchem.9b03259.
9. Forouzandeh, F.; Keypour, H.; Zebarjadian, M. H.; Mahmoudabadi, M.; Hosseinzadeh, L.; Karamian, R.; Khoei, M. A.; Gable, R. W. Synthesis, Characterization and X-Ray Crystal Structure of Potentially N_6O_2 Coordinating Macroacyclic Schiff Base Ligands and Their Mn(II), Zn(II) and Cd(II) Complexes; Cytotoxic, Antibacterial Properties and Competitive Li_7 NMR Studies. *Polyhedron* **2019**, *160*, 238–246. DOI: 10.1016/j.poly.2018.12.052.
10. Keypour, H.; Jamshidi, A. H.; Rezaeivala, M.; Valencia, L. Synthesis and Characterization of Mononuclear and Dimeric Ni(II), Cu(II) and Cd(II) Schiff Base Complexes with Two New

Asymmetrical Tripodal Amines. Crystal Structures of Ni(II) and Cd(II) Complexes and Their Antibacterial Studies. *Polyhedron* **2013**, *52*, 872–878. DOI: 10.1016/j.poly.2012.07.027.

11. Kynicky, J.; Milosavljevic, V.; Jelinkova, P.; Haddad, Y.; Rodrigo, M. A. M.; Buchtelova, H.; Bytesnikova, Z.; Brtnicky, M.; Richtera, L.; Kopel, P.; Adam, V. Europium and Terbium Schiff Base Peptide Complexes as Potential Antimicrobial Agents against *Salmonella typhimurium* and *Pseudomonas aeruginosa*. *Chem. Pap.* **2018**, *72*, 1437–1449. 0DOI: 10.1007/s11696-018-0400-3.
12. Hu, X. M.; Xue, L. W.; Zhao, G. Q.; Yang, W. C. Synthesis, Structures, and Biological Activity of Terbium(III) and Cobalt(III) Complexes Derived from Tripodal Schiff Bases. *Russ. J. Coord. Chem.* **2015**, *41*, 197–201. DOI: 10.1134/S1070328415030045.
13. Mukherjee, S.; Chaudhari, A. K.; Xue, S.; Tang, J.; Ghosh, S. K. An Asymmetrically Connected Hexanuclear Dy^{III}_6 Cluster Exhibiting Slow Magnetic Relaxation. *Inorg. Chem. Commun.* **2013**, *35*, 144–148. DOI: 10.1016/j.inoche.2013.06.027.
14. Mondal, K. C.; Kostakis, G. E.; Lan, Y.; Wernsdorfer, W.; Anson, C. E.; Powell, A. K. Defect-Dicubane Ni_2Ln_2 (Ln = Dy, Tb) Single Molecule Magnets. *Inorg. Chem.* **2011**, *50*, 11604–11611. DOI: 10.1021/ic2015397.
15. Ke, H.; Zhang, S.; Zhu, W.; Xie, G.; Chen, S. Synthesis, Structures, and Magnetic Properties of Four Dodecanuclear Ni_8RE_4 (RE = Gd, Dy, Y) Clusters Trapping Four μ_5-Bridged Carbonate Anions. *J. Coord. Chem.* **2015**, *68*, 808–822. DOI: 10.1080/00958972.2015.1004326.
16. Constable, E. C.; Housecroft, C. E.; Zampese, J. A.; Zhang, G. Multinuclear Zinc(II) Complexes with $\{Zn_6(\mu\text{-}O)_6(\mu_3\text{-}O)_2\}$- and $\{Zn_5(\mu\text{-}O)_3(\mu_3\text{-}O)_3\}$-Cluster Cores. *Polyhedron* **2012**, *44*, 150–155. DOI: 10.1016/j.poly.2012.06.033.
17. Griffiths, K.; Gallop, C. W. D.; Abdul-Sada, A.; Vargas, A.; Navarro, O.; Kostakis, G. E. Heteronuclear 3d/Dy^{III} Coordination Clusters as Catalysts in a Domino Reaction. *Chem. Eur. J.* **2015**, *21*, 6358–6361. DOI: 10.1002/chem.201500505.
18. Sheldrick, G. M. *SADABS Program for Empirical Absorption Correction of Area Detector*; University of Göttingen: Germany, **1996**.
19. Sheldrick, G. M. SHELXT – Integrated Space-Group and Crystal-Structure Determination. *Acta Crystallogr.* **2015**, *C71*, 3–8.
20. Saha, S.; Pal, S.; Gomez-Garcia, C. J.; Clemente-Juan, J. M.; Harms, K.; Nayek, H. P. A Ferromagnetic Tetranuclear Nickel(II) Schiff-Base Complex with an Asymmetric Ni_4O_4 Cubane Core. *Polyhedron* **2014**, *74*, 1–5. DOI: 10.1016/j.poly.2014.02.036.
21. Cindric, M.; Pavlovic, G.; Pajic, D.; Zadro, K.; Cincic, D.; Hrenar, T.; Leksic, E.; Prieto, A. B. P.; Lazic, P.; Jung, D. S. Correlation between Structural, Physical and Chemical Properties of Three New Tetranuclear Ni^{II} Clusters. *New J. Chem.* **2016**, *40*, 6604–6614. DOI: 10.1039/C6NJ00287K.
22. Li, J.; Wei, R.-M.; Pu, T.-C.; Cao, F.; Yang, L.; Han, Y.; Zhang, Y.-Q.; Zuo, J.-L.; Song, Y. Tuning Quantum Tunnelling of Magnetization through 3*d*-4*f* Magnetic Interactions: An Alternative Approach for Manipulating Single-Molecule Magnetism. *Inorg. Chem. Front.* **2017**, *4*, 114–122. DOI: 10.1039/C6QI00407E.
23. Chattopadhyay, S.; Bocelli, G.; Musatti, A.; Ghosh, A. First Oxidative Synthetic Route of a Novel, Linear Mixed Valence Co^{III}-Co^{II}-Co^{III} Complex with Bridging Acetate and Salen. *Inorg. Chem. Commun.* **2006**, *9*, 1053–1057. DOI: 10.1016/j.inoche.2006.06.017.
24. Majumder, A.; Rosair, G. M.; Mallick, A.; Chattopadhyay, N.; Mitra, S. Synthesis, Structures and Fluorescence of Nickel, Zinc and Cadmium Complexes with the *N,N,O*-Tridentate Schiff Base *N*-2-Pyridylmethylidene-2-Hydroxy-Phenylamine. *Polyhedron* **2006**, *25*, 1753–1762. DOI: 10.1016/j.poly.2005.11.029.
25. Gupta, N.; Swaroop, R.; Singh, R. V. Spectroscopic Characterization of Biologically Potent Hydrazinecarboxamides and Their Organoboron(III) Complexes. *Main Group Met. Chem.* **1997**, *14*, 387–392.
26. Chen, X.-M.; Tong, Y.-X.; Mak, T. C. W. A Dinuclear Zinc Carboxylate Complex of Biological Relevance – Crystal-Structure of $[Zn_2(Bpy)_2(MeCO_2)_3]ClO_4$ (bpy = 2,2'-bipyridine.). *Inorg. Chem.* **1994**, *33*, 4586–4588. DOI: 10.1021/ic00098a029.
27. Srivastava, R. S. Pseudotetrahedral Co(II), Ni(II) and Cu(II) Complexes of N1-(o-Chlorophenyl)-2-(2',4'-Dihydroxyphenyl)-2-Benzylazomethine Their Fungicidal and Herbicidal Activity. *Inorg. Chim. Acta* **1981**, *56*, L65–L67. DOI: 10.1016/S0020-1693(00)88534-5.
28. Levinson, W.; Jawetz, E. *Medical Microbiology and Immunology*, 4th ed.; Springer-Verlag: Stamford, **1996**.